

Controllable Incremental Algorithm for Entanglement Entropy and Other Observables with Exponential Variance Explosion in Many-Body Systems

Yuan Da Liao^{1,2}

¹State Key Laboratory of Surface Physics, Fudan University, Shanghai 200438, China

²Center for Field Theory and Particle Physics, Department of Physics, Fudan University, Shanghai 200433, China

(Dated: July 21, 2023)

Researchers in the field of physical science are continuously searching for universal features in strongly interacting many-body systems. However, these features can often be concealed within highly complex observables, such as entanglement entropy (EE). The non-local nature of these observables makes them challenging to measure experimentally or evaluate numerically. Therefore, it is of utmost importance to develop a reliable and convenient algorithm that can accurately obtain these complex observables. In this paper, with help of quantum Monte Carlo (QMC), we reveal that the statistical variance of EE exponentially explodes with respect to the system size, making the evaluation of EE inaccurate. We further introduce an incremental algorithm based on the framework of QMC to solve this conundrum. The total number of our incremental processes can be quantitatively determined and reasonably adjusted, making it easy to control the precision in practice. We demonstrate the effectiveness and convenience of our incremental algorithm by using it to obtain the highly accurate EE of a 2D Hubbard model as an example. Additionally, our algorithm can be potentially generalized to calculate other numerically statistically unstable observables with exponential variance growth, such as the entanglement spectrum and topological entanglement negativity of correlated boson/spin and fermion systems, as well as other general functions of determinants of Green's functions in interacting fermions. Accurately measuring these complex observables has the potential to inspire the development of physical theories and guide the direction of experiments.

Introduction.— Physical science researchers are always seeking for the universal properties in correlated many-body systems [1, 2]. These properties can be difficult to detect because they are often hidden within complex observables that have a non-local nature, which means that it is hard to measure them experimentally or to even evaluate them numerically. One example of such an observable is the entanglement entropy (EE), that is a measure of the information entanglement of the boundary of subsystems [3, 4]. The EE generally shows a finite-size scaling relation, and the corresponding scaling coefficients, that are related to the low-energy physics and subsystem geometry of studied systems, can manifest such universal features.

For instance, in one-dimensional critical systems, it has been proven that the EE scales logarithmically with respect to the subsystem size and has a universal leading coefficient proportional to the central charge [5–7]. In two and higher dimensions, although the theory of calculating EE is not completely known, there is a consensus that EE grows proportionally to the area of the subsystem boundary for both critical and non-critical systems [3], which is referred to as the well-known "area law" scaling. Interestingly, for critical systems, a subleading universal and geometry-dependent logarithmic coefficient will be displayed [4, 8], as is the case for free Dirac cones [9] and quantum critical points (QCPs) [10, 11]. Furthermore, due to the interaction of Goldstone modes and the restoration of symmetry in a limited space, a universal subleading logarithmic coefficient will arise [12]. This coefficient is equal to half the number of Goldstone modes and applies to both spin and fermion models with continuous spontaneous symmetry breaking [8, 10, 11, 13–17]. All these intriguing facts represent that the EE can be a potent tool for revealing

the universal features of critical systems.

The theoretical explanation of the universal coefficients of the n -th Rényi EE beyond the area law scaling for free Dirac fermions in 2D has become apparently clear [1, 9]. However, for interacting fermions, the complete theoretical understanding is not yet well-established. Therefore, a viable alternative to extract the universal features of the EE for interacting fermions is the use of numerical tools. The auxiliary-field determinant quantum Monte Carlo (DQMC) simulation is a suitable and unbiased numerical method to study the properties of interacting fermions. In recent years, significant algorithmic advances have been made. Grover's pioneering work [18] presented a seminal numerical definition of the 2nd Rényi EE S_2^A for interacting fermions within the DQMC framework, here A is the entangled region we choose, as shown in Fig. 1(c). This definition is given by $e^{-S_2^A} = \langle \det g_A^{s_1, s_2} \rangle$, and a matrix $g_A^{s_1, s_2}$, that relates to two independent replica configurations of the auxiliary field $\{s_1\}$ and $\{s_2\}$, is introduced. However, direct statistics of the determinant of Grover's matrix $g_A^{s_1, s_2}$ suffer from severe instability at slightly stronger coupling and slightly larger subsystem sizes [16], which prevents accurate calculation of the EE [19, 20].

Over the past decade, many attempts have been made to solve this problem [10, 21, 22], but none have achieved a perfect solution. Methods used a few years ago involved introducing an extra entangling subsystem that effectively enlarged the total system size, which offered better controlled statistical errors but became cumbersome in practical simulations [21, 22]. Similar dilemma also exists in the boson/spin system [23–27]. And it is an urgency to pave the way to more common algorithm to deal with such predicaments. Recently, incremental methods based on QMC have been developed for

boson/spin system [14] and interacting fermions [10]. These methods have been used to successfully extracted the universal logarithmic coefficients of the 2nd Rényi EE for the Gross-Neveu QCP [10], deconfined QCP [11, 28], and Goldstone model [10, 11, 15, 16] with unprecedented precision, which is undoubtedly a significant breakthrough. However, in fermions case, the incremental method introduces an additional configuration space that results in an increased computational burden. Additionally, the updating strategy for balancing the inherent auxiliary fields and the additional configuration becomes more difficult to define. Moreover, the total number of the incremental process generally needs to be quite large and often be estimated empirically instead of being quantitatively determined. These limitations render such incremental method difficult to apply in practical situations and there is an urgent need for the development of improved methods.

In this paper, we develop an improved incremental method for computing the Rényi EE of interacting fermions. Unlike existing methods [10, 18, 21, 22], our approach does not suffer from the aforementioned issues. Notably, our method does not require additional configuration space, and the total number of incremental procedures is not only relatively fewer than the method introduced in Ref. [10], but also can be quantitatively determined. Moreover, our method can be easily extended to calculate other physical observables such as the entanglement spectrum and topological entanglement negativity of correlated boson/spin and fermion systems, and other general functional of determinants of Green functions in interacting fermions.

Model and Methods details.— In this paper, we investigate the zero-flux Hubbard model on a square lattice at half-filling to showcase the effectiveness and convenience of our improved incremental method. The Hamiltonian of the model is given by

$$H = -t \sum_{\langle ij \rangle} \left(c_{i\sigma}^\dagger c_{j\sigma} + \text{h.c.} \right) + U \sum_i n_{i\uparrow} n_{i\downarrow} \quad (1)$$

where $c_{i\sigma}^\dagger$ and $c_{i\sigma}$ represent the creation and annihilation operators with spin $\sigma = \uparrow, \downarrow$ on site i , $\langle ij \rangle$ denote the nearest neighbor hopping, $n_{i\sigma} = c_{i\sigma}^\dagger c_{i\sigma}$ is the particle number operator for spin σ . We set $t = 1$ as the energy unit. When U is finite, the ground state is the well-known antiferromagnet, a strongly correlated Mott insulator state. We employ our improved incremental method to calculate the 2nd Rényi EE at $U/t = 10$.

The explicit numerical definition of 2nd Rényi EE proposed by Grover [18] is as follows

$$e^{-S_2^A} = \frac{\sum_{\{s_1\}, \{s_2\}} W_{s_1} W_{s_2} \det g_A^{s_1, s_2}}{\sum_{\{s_1\}, \{s_2\}} W_{s_1} W_{s_2}}, \quad (2)$$

where W_s represents the unnormalized weight of configuration $\{s\}$, Grover matrix, defined as $g_A^{s_1, s_2} = G_A^{s_1} G_A^{s_2} + (\mathbb{I} - G_A^{s_1})(\mathbb{I} - G_A^{s_2})$, is a functional of Green's functions $G_A^{s_1}$ and $G_A^{s_2}$ of two independent replica. Directly measuring $\langle \det g_A^{s_1, s_2} \rangle$ becomes extremely unstable at slightly stronger

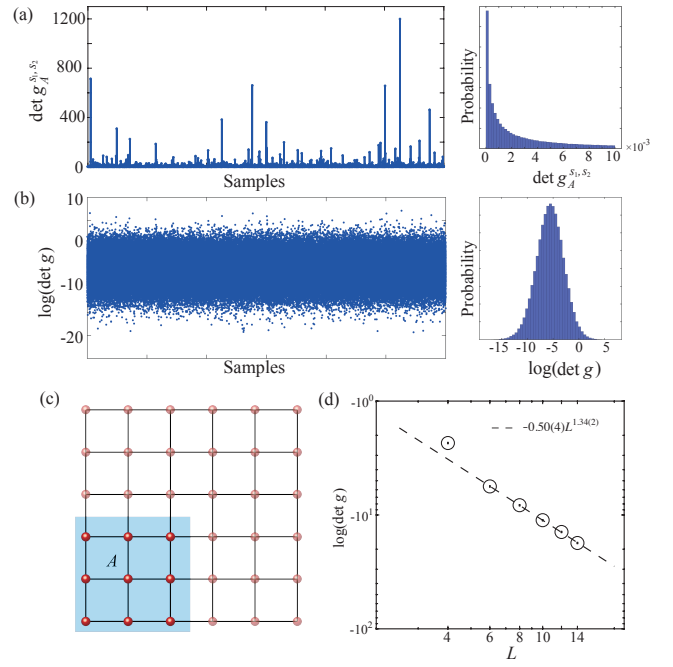


FIG. 1. (a) and (b) show the sampling distributions and normalized histograms of $\det g_A^{s_1, s_2}$ and $\log(\det g)$. We notice that the statistical distribution of $\log(\det g)$ conforms to the normal form, while $\det g_A^{s_1, s_2}$ apparently not. (c) The square lattice we used, and the blue region A is our chosen entanglement region with $L/2 \times L/2$ sites. (d) The log-log plot of $\log(\det g)$ as function of system size L , the data can be fit with a perfect scaling relation $\log(\det g) = -0.95(5)L^{1.35(2)}$. Error bars are smaller than the symbols.

coupling and larger sizes [16]. This is due to the fact that the distribution of $\det g_A^{s_1, s_2}$ becomes very broad with rare spikes, as shown in Fig. 1 (a). However, these rare events significantly impact the expectation value of $\det g_A^{s_1, s_2}$. D'Emidio et al [10] think that the rare events dominate the statistical average and the probability of sampling these rare events could increase if $\det g_A^{s_1, s_2}$ is included in the weight of DQMC updating. Based on this understanding, they developed an incremental method to obtain a reliable EE, which is given by

$$e^{-S_2^A} = \frac{Z(\lambda_1)}{Z(\lambda_0 = 0)} \frac{Z(\lambda_2)}{Z(\lambda_1)} \cdots \frac{Z(\lambda_{k+1})}{Z(\lambda_k)} \cdots \frac{Z(\lambda_{N_\lambda} = 1)}{Z(\lambda_{N_\lambda-1})}, \quad (3)$$

where the integer k represents k -th incremental process, the real number λ_k grows from 0 to 1. The replicated partition function is defined as

$$Z(\lambda_k) = \sum_{\{s_1, s_2, C \subseteq A\}} \lambda_k^{N_C} (1 - \lambda_k)^{N_A - N_C} W_{s_1} W_{s_2} \det g_C^{s_1, s_2}, \quad (4)$$

where C are proper subsets of the entanglement region A , N_C (N_A) is the number of sites in region C (A), and $Z(\lambda_0 = 0) = \sum_{\{s_1\}, \{s_2\}} W_{s_1} W_{s_2}$ and $Z(\lambda_{N_\lambda} = 1) = \sum_{\{s_1\}, \{s_2\}} W_{s_1} W_{s_2} \det g_A^{s_1, s_2}$ make Eq. (3) satisfy the initial definition (2) of 2nd Rényi EE. By simple formula derivation, each

incremental process is given by

$$\frac{Z(\lambda_{k+1})}{Z(\lambda_k)} = \frac{\sum_{\{s_1, s_2, C \subseteq A\}} \mathbf{W}_{C, \lambda_k}^{s_1, s_2} O_{\lambda_k, \lambda_{k+1}}}{\sum_{\{s_1, s_2, C \subseteq A\}} \mathbf{W}_{C, \lambda_k}^{s_1, s_2}}, \quad (5)$$

where the replaced sampling weight $\mathbf{W}_{C, \lambda_k}^{s_1, s_2} = \lambda_k^{N_C} (1 - \lambda_k)^{N_A - N_C} W_{s_1} W_{s_2} \det g_A^{s_1, s_2}$, and the replaced sampling observable $O_{\lambda_k, \lambda_{k+1}} = (\lambda_{k+1}/\lambda_k)^{N_C} [(1 - \lambda_{k+1})/(1 - \lambda_k)]^{N_A - N_C}$. It's worth to notice that the replaced sampling weight includes $\det g_A^{s_1, s_2}$, and the replaced sampling observable becomes the power function of the ratios λ_{k+1}/λ_k and $(1 - \lambda_{k+1})/(1 - \lambda_k)$. If the incremental process is slow enough, $\langle O_{\lambda_k, \lambda_{k+1}} \rangle$ would scale of unity and be evaluated accurately, resulting in a reliable estimate of EE. That is undoubtedly a significant breakthrough, however, an additional configuration space $C \subseteq A$ has to be included, and in practice, $N_\lambda \sim 50$ [11, 16] estimated empirically, which significantly increases the computational burden. We appreciate the approach they have developed to achieve statistical observable scaling to unity, which resulting in pretty accurate EE. However, it is not possible to quantitatively determine the total number N_λ of incremental processes in their method. In practice, one must estimate N_λ empirically, which results in imprecise EE values if the chosen value of N_λ is not sufficiently large. Unfortunately, there is no clear indication of how large N_λ needs to be to ensure accurate EE values. Additionally, we also don't quantitatively know how often one need to update additional configurations and how to balance it with the inherent auxiliary fields of DQMC.

These limitations motivate us to search for an alternative algorithm. Interestingly, as shown in Fig. 1 (b), we observed that the logarithm of $\det g_A^{s_1, s_2}$, aliased as $\log(\det g)$, conforms very well to a normal distribution, making it possible to accurately evaluate it using Grover's method. In addition, as shown in Fig. 1 (d), $\langle \log(\det g) \rangle$ follows a power function of the perfect form aL^γ , $a = -0.50(4)$ and $\gamma = 1.34(2)$ in our case, which implies that the statistical variance of $\langle \log(\det g) \rangle$ grows polynomially relative to L , i.e., $\delta[\log(\det g)] \sim L^\gamma$. However, the variance of $\det g_A^{s_1, s_2}$ would disastrously exponentially grow as $\delta[\det g_A^{s_1, s_2}] \sim L^\gamma e^{L^\gamma}$. According to the central limit theorem, the exponentially increased computational burden cannot be afforded in order to achieve an accurate estimate of $\det g_A^{s_1, s_2}$ as the system size increases. This is why we failed to calculate the EE directly according to Eq. (2). Fortunately, in principle, the variance of $(\det g_A^{s_1, s_2})^{1/N_\lambda}$ should grow as $\delta[(\det g_A^{s_1, s_2})^{1/N_\lambda}] \sim \frac{L^\gamma}{N_\lambda} e^{L^\gamma/N_\lambda}$. If we intelligently set $N_\lambda \sim L^\gamma$, then $\delta[(\det g_A^{s_1, s_2})^{1/N_\lambda}] \sim e$, and thus $\langle (\det g_A^{s_1, s_2})^{1/N_\lambda} \rangle$ can be reasonably evaluate very well.

Based on our observations and reasoning, we introduce an improved incremental method using Eq. (3), as follows

$$Z(\lambda_k) = \sum_{\{s_1, s_2\}} W_{s_1} W_{s_2} W(\lambda_k, \det g_A^{s_1, s_2}), \quad (6)$$

where $W(\lambda_k, \det g_A^{s_1, s_2}) = (\det g_A^{s_1, s_2})^{\lambda_k}$ with $\lambda_k = k/N_\lambda$, $Z(\lambda_0 = 0) = \sum_{\{s_1, s_2\}} W_{s_1} W_{s_2}$ and $Z(\lambda_{N_\lambda} = 1) =$

$\sum_{\{s_1, s_2\}} W_{s_1} W_{s_2} \det g_A^{s_1, s_2}$ naturally satisfy the initial definition (2) of 2nd Rényi EE. Now, each incremental process can be evaluated in parallel as follows

$$\frac{Z(\lambda_{k+1})}{Z(\lambda_k)} = \frac{\sum_{\{s_1, s_2\}} W_{s_1} W_{s_2} (\det g_A^{s_1, s_2})^{\lambda_k} (\det g_A^{s_1, s_2})^{1/N_\lambda}}{\sum_{\{s_1, s_2\}} W_{s_1} W_{s_2} (\det g_A^{s_1, s_2})^{\lambda_k}}, \quad (7)$$

where N_λ is quantitatively determined as the nearest integer greater than or equal to $|\langle \log(\det g) \rangle|$, i.e. $N_\lambda \simeq 0.5L^{1.34}$ in our case. Then $\delta[(\det g_A^{s_1, s_2})^{1/N_\lambda}] \sim 1$, and $\frac{Z(\lambda_{k+1})}{Z(\lambda_k)}$ can be reasonably evaluated reliably. Furthermore, our improved method doesn't require any additional configuration space, which would otherwise escalate the computational burden.

Since Rényi EE is a zero-temperature physical quantity, it is high suitable to incorporate our improved incremental algorithm into the projector DQMC method. The method's details can be found in our previous works [11, 16], and we will only mention that the projection length β is set to the system size L , and a discrete time slice is set to 0.1. We simulated systems with linear sizes $L = 2, 4, 6, 9, 10, 12$ and 14. The computational complexity of each incremental process remains $O(\beta L^6)$, the same as that of the standard DQMC method. The overall computational complexity of computing the EE is $O(\beta L^{6+\gamma})$, because of the $N_\lambda \sim L^\gamma$ incremental steps required. Nevertheless, these steps can be evaluated in parallel, thereby enabling us to obtain a reliable 2nd Rényi EE using the same computational time as the standard DQMC.

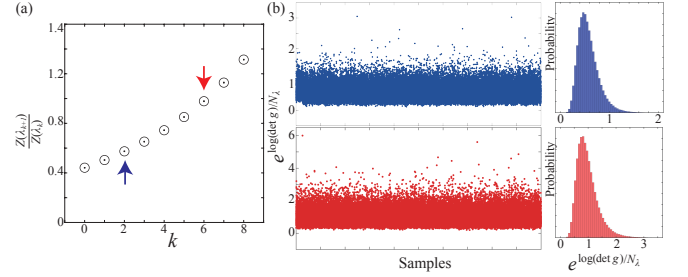


FIG. 2. (a). The $\frac{Z(\lambda_{k+1})}{Z(\lambda_k)}$ as function of incremental process for $U/t = 10$ and $L = 8$. Here N_λ is 9. We can notice that the $\frac{Z(\lambda_{k+1})}{Z(\lambda_k)}$ of each k -th process can be evaluated very well, which will give rise to reliable and accurate 2nd Rényi EE. (b) The sampling distributions and normalized histograms of new observable of our improved algorithm $e^{\log(\det g)/N_\lambda}$. All pieces of incremental process generate reliable samples of $e^{\log(\det g)/N_\lambda}$ that approximatively follow normal distribution and can be reasonably estimate.

Numerical results.— As we mentioned above, Fig. 1 (a) and (b) exhibit the sampling distributions and normalized histograms of $\det g_A^{s_1, s_2}$ and $\log(\det g)$, respectively. The distribution of $\det g_A^{s_1, s_2}$ shows infrequent spikes, and it is clear that the corresponding histogram does not conform to a Gaussian form. This phenomenon has been observed previously in Ref. [16]. On the other hand, the samples of $\log(\det g)$ are normally distributed, allowing us to estimate $\langle \log(\det g) \rangle$ and the associated statistical errors reasonably. As shown in Fig. 1 (d), $\langle \log(\det g) \rangle$ grows in the perfect

form of a power function with respect to L . Our fitting result is $\langle \log(\det g) \rangle = -0.50(4)L^{1.34(2)}$. This scaling behavior explains why instability becomes more noticeable for larger system sizes. Because the statistical variance of determinant of Grover matrix will exponentially explode. Whether the prefactor and power coefficient are universal remains an open question. Nevertheless, this scaling behavior can be used to determine the value of N_λ for various values of L , including larger ones, without the requirement of more calculations. Here, according to $N_\lambda \simeq 0.5L^{1.34}$, we quantitatively determined the corresponding N_λ values as $N_\lambda = 6, 9, 12, 15$ and 18 for $L = 6, 8, 10, 12$ and 14, based on the data shown in Fig. 1 (d).

Our improved incremental method allows us to evaluate the new observables $(\det g_A^{s_1, s_2})^{1/N_\lambda}$ for each piece of parallel incremental process with controlled statistical errors, as illustrated in Fig. 2(a). As expected, all pieces of the incremental process generate reliable samples that approximately follow a normal distribution and have a finite variance. To demonstrate this, we have selected two parallel pieces and plotted their sample distributions and histograms in Fig. 2(b).

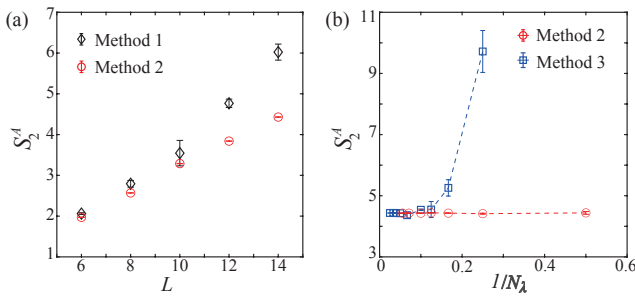


FIG. 3. (a) The 2nd Rényi EE obtained with method developed by Grover (Method 1) [18] and in this paper (Method 2). (b) The $1/N_\lambda$ extrapolation of EE with $L = 14$ for method developed by D’Emidio et al (Method 3) [18] and Method 2. It is important to note that the errorbars of data obtained with Method 1 are not credible, because the mean values of Method 1 don’t converge in principle.

According to Eq. (3), the reliable 2nd Rényi EE can be obtained by multiplying all parallel expected values $\frac{Z(\lambda_{k+1})}{Z(\lambda_k)}$ together. As shown in Fig. 3, we compare the estimates of the 2nd Rényi EE using the method developed by Grover (Method 1) [18], our method (Method 2), and the method developed by D’Emidio et al (Method 3) [10], within comparable CPU times. As shown in Fig. 3(a), the results obtained with Method 1 obviously deviate from the reliable values for $L > 6$, and this deviation becomes more noticeable as the system sizes increase. It is important to note that the errorbars of data obtained with Method 1 are not credible, because the mean values of Method 1 don’t converge in principle. Instead, we don’t need to force $N_\lambda \simeq |aL^\gamma|$, we can adjust N_λ to balance precision and computational burden. For example, if we choose $N_\lambda \simeq 0.5|aL^\gamma|$ then $\delta[(\det g_A^{s_1, s_2})^{1/N_\lambda}] \sim 2e^2$, and we can halve our total CPU time while still obtaining pretty accurate results of EE in principle.

As shown in Fig. 3(b), we plot the $1/N_\lambda$ extrapolation of the 2nd Rényi EE for $L = 14$ with Method 2. The values of EE become relatively less accurate, but the deviation is not significant. Furthermore, we compare the estimate of 2nd Rényi EE with Method 2 and Method 3 for different N_λ . As N_λ increases, the results obtained with Method 2 and Method 3 gradually converge. When $N_\lambda \rightarrow \infty$, Method 2 and Method 3 give consistent evaluated values of EE. However, Method 3 requires much larger N_λ to achieve the accuracy of Method 2. Unfortunately, there is no clear indication of the imprecision of Method 3 if we do not make such a comparison, as shown in Fig. 3(b). This makes Method 2 less convenient and reliable in practice. Therefore, Method 3 should perform better in practice.

Discussions.— We have devised an improved incremental algorithm for the 2nd Rényi EE within the DQMC framework. Our algorithm is highly effective due to the reduction of variance in sampling, which goes from an exponential growth to a polynomial one, based on the observation that the logarithm of the determinant of the Grover matrix can be reasonably evaluated. Consequently, the total number of incremental processes, denoted as N_λ , can be quantitatively determined, and our algorithm doesn’t introduce any additional configuration space that will increase computational burden. Furthermore, each incremental process can be performed in parallel, keeping the computational time the same as the standard DQMC method. Moreover, N_λ can be adjusted reasonably to strike a balance between calculation accuracy and CPU computational burden. These benefits make our algorithm practical for use in research. Additionally, our method can be extended to calculate other complex physical observables, such as the entanglement spectrum and topological entanglement negativity of correlated boson/spin systems, other general functional of determinants of Green’s functions in interacting fermions, because these observables also suffer exponential growth of statistical variance. In fact, our method can be applied to any physical quantity, as long as the variance of this quantity is statistically exponentially enlarging, but its logarithm follows a normal distribution in DQMC or others QMC framework. Accurately measuring these elusive observables has the potential to inspire the development of physical theories and guide the direction of experiments.

Acknowledgements — We thank Zi Yang Meng, Yang Qi, Zheng Yan and Xiao Yan Xu for helpful discussions. We acknowledge support from National Natural Science Foundation of China (Grant No. 12247114) and the China Postdoctoral Science Foundation (Grants Nos. 2021M700857 and 2021TQ0076).

[1] I. R. Klebanov, S. S. Pufu, S. Sachdev, and B. R. Safdi, *Journal of High Energy Physics* **2012**, 74 (2012).
[2] E. Altman and R. Vosk, *Annual Review of Condensed Matter Physics* **6**, 383 (2015).
[3] J. Eisert, M. Cramer, and M. B. Plenio, *Reviews of Modern*

Physics **82**, 277 (2010).

[4] H. Casini and M. Huerta, Nuclear Physics B **764**, 183 (2007).

[5] G. Vidal, J. I. Latorre, E. Rico, and A. Kitaev, Physical Review Letters **90**, 227902 (2003).

[6] P. Calabrese and J. Cardy, Journal of Statistical Mechanics: Theory and Experiment **2004**, P06002 (2004).

[7] V. E. Korepin, Physical Review Letters **92**, 096402 (2004).

[8] H. F. Song, N. Laflorencie, S. Rachel, and K. Le Hur, Physical Review B **83**, 224410 (2011).

[9] J. Helmes, L. E. Hayward Sierens, A. Chandran, W. Witczak-Krempa, and R. G. Melko, Physical Review B **94**, 125142 (2016).

[10] J. D'Emidio, R. Orus, N. Laflorencie, and F. de Juan, Universal features of entanglement entropy in the honeycomb Hubbard model (2022), arxiv:2211.04334.

[11] Y. Da Liao, G. Pan, W. Jiang, Y. Qi, and Z. Y. Meng, The teaching from entanglement: 2D deconfined quantum critical points are not conformal (2023), arxiv:2302.11742 [cond-mat, physics:math-ph, physics:physics, physics:quant-ph].

[12] M. A. Metlitski and T. Grover, Entanglement entropy of systems with spontaneously broken continuous symmetry (2015), arXiv:1112.5166 [cond-mat.str-el].

[13] A. B. Kallin, M. B. Hastings, R. G. Melko, and R. R. P. Singh, Physical Review B **84**, 165134 (2011).

[14] J. D'Emidio, Physical Review Letters **124**, 110602 (2020).

[15] J. Zhao, B.-B. Chen, Y.-C. Wang, Z. Yan, M. Cheng, and Z. Y. Meng, npj Quantum Materials **7**, 69 (2022).

[16] G. Pan, Y. Da Liao, W. Jiang, J. D'Emidio, Y. Qi, and Z. Y. Meng, Computing entanglement entropy of interacting fermions with quantum Monte Carlo: Why we failed and how to get it right (2023), arxiv:2303.14326 [cond-mat, physics:math-ph, physics:physics, physics:quant-ph].

[17] Z. Deng, L. Liu, W. Guo, and H. Q. Lin, Improved scaling of the entanglement entropy of quantum antiferromagnetic Heisenberg systems (2023), arxiv:2306.01554 [cond-mat].

[18] T. Grover, Physical Review Letters **111**, 130402 (2013).

[19] C.-C. Chang, R. R. P. Singh, and R. T. Scalettar, Physical Review B **90**, 155113 (2014).

[20] F. F. Assaad, T. C. Lang, and F. Parisen Toldin, Physical Review B **89**, 125121 (2014).

[21] P. Broecker and S. Trebst, Journal of Statistical Mechanics: Theory and Experiment **2014**, P08015 (2014).

[22] L. Wang and M. Troyer, Physical Review Letters **113**, 110401 (2014).

[23] R. G. Melko, A. B. Kallin, and M. B. Hastings, Physical Review B **82**, 100409 (2010).

[24] M. B. Hastings, I. González, A. B. Kallin, and R. G. Melko, Physical Review Letters **104**, 157201 (2010).

[25] S. Hohenruh and T. Roscilde, Physical Review B **86**, 235116 (2012).

[26] D. J. Luitz, X. Plat, N. Laflorencie, and F. Alet, Physical Review B **90**, 125105 (2014).

[27] B. Kulchytskyy, C. M. Herdman, S. Inglis, and R. G. Melko, Phys. Rev. B **92**, 115146 (2015).

[28] J. Zhao, Y.-C. Wang, Z. Yan, M. Cheng, and Z. Y. Meng, Phys. Rev. Lett. **128**, 010601 (2022).